

Heavy dibaryons $\Xi_{cc}^{(*)}\Xi_{cc}^{(*)}$ and $\Xi_{bb}^{(*)}\Xi_{bb}^{(*)}$

An-Su Lu, Mao-Jun Yan*, Chun-Sheng An†, and Cheng-Rong Deng‡

^a*School of Physical Science and Technology, Southwest University, Chongqing 400715, China*

We systematically investigate the dibaryons $\Xi_{cc}^{(*)}\Xi_{cc}^{(*)}$ (di- Ξ_{cc}) and $\Xi_{bb}^{(*)}\Xi_{bb}^{(*)}$ (di- Ξ_{bb}), with various isospin-spin configurations $I(J^P)$ in a nonrelativistic quark model. For the di- Ξ_{cc} system, only the single channels $\Xi_{cc}\Xi_{cc}^*$ and $\Xi_{cc}^*\Xi_{cc}^*$ with $0(1^+)$ are capable of forming deuteronlike bound states, with the σ meson exchange playing a decisive role. Those states have binding energies of approximately -1.5 MeV and -3.3 MeV and sizes of 2.37 fm and 1.87 fm, respectively. The coupled channel effect in the di- Ξ_{cc} system with $0(1^+)$ enhances the attraction. As a result, this di- Ξ_{cc} system can establish a deuteronlike configuration, with the binding energy of -7.5 MeV relative to the threshold $\Xi_{cc}\Xi_{cc}$ and the size of approximately 1.40 fm. For the di- Ξ_{bb} system, the single channels with $0(1^+)$, $0(2^+)$, and $0(3^+)$ can give rise to deuteronlike bound states with binding energies ranging from -6.1 MeV to -14.3 MeV. Additionally, the di- Ξ_{bb} system with $1(0^+)$ and $1(2^+)$ can also establish deuteronlike bound states with binding energies of around -0.5 MeV. When considering the coupled channel effect in the di- Ξ_{bb} system with $0(1^+)$, a compact hexaquark state is formed, exhibiting a binding energy of -21.2 MeV relative to the threshold $\Xi_{bb}\Xi_{bb}$ and a size of 0.53 fm. In this state, the π meson exchange provides a very powerful attractive force. The meson exchange interactions in the quark model is dispensable in the di- Ξ_{bb} bound states, except for $\Xi_{bb}^*\Xi_{bb}^*$ with $1(0^+)$.

I. INTRODUCTION

A dibaryon is defined as a system with a baryon number $B = 2$, composed of six valence quarks. These quarks can manifest in two forms: either as a loosely baryon-baryon configuration or as a tightly bound, spatially compact hexaquark state. The best-known dibaryon, the deuteron, is a loosely bound system composed of a proton and a neutron [1], whereas the state $d^*(2380)$ is widely regarded as a compact hexaquark state because of its large binding energy relative to the threshold $\Delta\Delta$ [2–4]. Alternatively, the state $d^*(2380)$ is described as a $\mathcal{D}_{12}\pi$ configuration with the pion in relative P-wave [5, 6]. Deuteronlike hadronic molecules have emerged as the leading interpretation for the internal structure of the so-called XYZ , P_c , P_{cs} , T_{cc} and T_{cs} states [7–14]. It is therefore natural to explore similar dibaryons [15–28], which contain one or more heavy quarks in their valence structure, and to search for their discovery when the requisite center-of-momentum energy and luminosity become accessible at experimental facilities.

The Heavy Diquark-Antiquark Symmetry (HADS) posits that the heavy quark pair $[QQ]$, confined in the color $\mathbf{3}$ state within doubly heavy baryons, forms a compact object due to the strong attractive color Coulomb interaction [29]. In the heavy quark limit, the heavy diquark $[QQ]$ behaves as a point-like particle, acting purely as a static color source in the $\bar{\mathbf{3}}$ channel. The HADS facilitates the establishment of a correlation between the doubly heavy baryons QQq ($\bar{Q}\bar{Q}\bar{q}$) and singly heavy mesons $\bar{Q}q$ ($Q\bar{q}$). Building on the molecular assumption for the P_c states, the existences of bound tri-charmed dibaryons,

$\Xi_{cc}^{(*)}\Sigma_c^{(*)}$, as well as the hexaquark molecule composed of a tetraquark state $T_{\bar{c}\bar{c}}$ and \bar{D}^* have been predicted within the HADS framework [30–33].

The characteristic size of the doubly charmed state $T_{cc}^+(3875)$ reported by the LHCb Collaboration suggests its deuteron-like molecular configuration, specifically DD^* [34, 35]. In the wake of this discovery, theorists proposed a wide range of possible tetraquark partners within various theoretical frameworks [36–51]. According to the HADS, the dibaryon partners, $\Xi_{cc}^{(*)}\Xi_{cc}^{(*)}$ (which is equivalent to $\Xi_{cc}^{(*)}\Xi_{cc}^{(*)}$), which are derived by replacing a c -quark in the state $T_{cc}^+(3875)$ with a diquark $[\bar{c}\bar{c}]$, could produce a bound deuteron-like dibaryon.

According to the heavy quark flavor symmetry (HQFS), the observation of $T_{cc}^+(3875)$ suggests that its bottom counterpart, T_{bb}^- with 01^+ , should exist. The existing studies indicated that the state T_{bb}^- with 01^+ is more stable bound state compared to $T_{cc}^+(3875)$ [38, 52]. Furthermore, the double bottom baryon Ξ_{bb} is anticipated to be observed in the near future [53]. However, the production of such states in experiments poses significant challenges. Similar to the state di- Ξ_{cc} , the di- Ξ_{bb} configuration may also give rise to the formation of bound states. Although the doubly bottom baryon $\Xi_{bb}^{(*)}$ has yet to be observed experimentally, its theoretical predictions suggest intriguing possibilities for future discoveries in the field of hadronic physics.

Experimental data concerning interactions between two heavy baryons is quite limited due to the challenges associated with generating two heavy baryons in laboratory settings. On the lattice quantum chromodynamics (LQCD) side, several heavy flavor dibaryon states have been studied [24–28], including di- Ω_{ccc} , di- Ω_{bbb} , di- Λ_c , di- Σ_c , $\Sigma_c\Xi_{cc}$, $\Omega_{cc}\Omega_c$, $\Omega_{bb}\Omega_b$, and $\Omega_{cbb}\Omega_{ccb}$. These studies have predicted the existence of several bound states within these systems. However, it is noteworthy that the dibaryon states di- Ξ_{cc} and di- Ξ_{bb} remain under ex-

*yanmj0789@swu.edu.cn

†ancs@swu.edu.cn

‡crdeng@swu.edu.cn

explored in LQCD research. Up to now, only the one-boson-exchange (OBE) model has explored the state $\text{di-}\Xi_{cc}$, predicting the existence of several potential bound states [16, 17]. In contrast, there has been no any theoretical researches on the state $\text{di-}\Xi_{bb}$.

In this study, we aim to conduct a systematic investigation of the properties of the heavy dibaryons $\text{di-}\Xi_{cc}$ and $\text{di-}\Xi_{bb}$. We will analyze a range of isospin-spin configurations in order to identify potential bound states within the framework of the quark model. We will investigate their binding energies, underlying binding mechanisms, and spatial structures. With this model, our previous work has investigated the natures of the single flavored dibaryon $\text{di-}\Delta$, $\text{di-}\Omega$, $\text{di-}\Omega_{ccc}$, and $\text{di-}\Omega_{bbb}$ [20]. The primary objective of this work is to deepen our understanding of the properties and structures of heavy dibaryon states from a phenomenological perspective. We aim to provide valuable insights that can inform future experimental endeavors aimed at identifying these dibaryon states. In addition, we will investigate the fundamental binding mechanisms that contribute to the formation and stability of these bound states. Our research seeks to uncover evidence for binding mechanisms that are unique to these systems, thereby enhancing our comprehension of the dynamics of heavy quarks and the meson-exchange interactions among light quarks. This exploration will yield important insights into the fundamental forces that govern the behavior of heavy dibaryons.

Following the introduction, the paper is organized as follows: In Sec. II, we present the quark model Hamiltonian. In Sec. III, we provide a brief overview of the wave functions for ground-state dibaryons. In Sec. IV, we present the numerical results and discussions. Finally, the paper concludes with a brief summary in Sec. V.

II. THEORETICAL FRAMEWORKS

Quantum Chromodynamics (QCD) is widely regarded as the fundamental theory of strong interaction, governing the dynamics of quarks and gluons. At the hadron scale, QCD exhibits highly nonperturbative behavior due to the intricate infrared dynamics of the non-Abelian SU(3) gauge group. Direct calculations of hadron spectra and hadron-hadron interactions from first principles in QCD remain extremely challenging. As a result, a less rigorous yet highly effective approach the QCD-inspired quark models serve as a powerful tool for gaining physical insight into these complex strong-interaction systems. The quark models are based on the assumption that hadrons are color-singlet, nonrelativistic bound states of constituent quarks, with phenomenologically derived effective masses and interactions. These models were developed based on a comprehensive understanding of the

nature of baryons and the nucleon-nucleon interactions.

The naive quark model (Isgur-Karl model) typically includes an effective one-gluon-exchange (OGE) potential, V^{oge} , which directly stems from the one-gluon exchange diagram in QCD [54], and an artificial quark confinement potential, V^{con} . This model offers an excellent description of light baryons [55, 56]. In the context of nucleon-nucleon interactions, the model can capture the short-range repulsive core via the spin-spin component of the inter-quark interaction between nucleons, as well as the Pauli exclusion principle, which is enforced by the quark structure of the nucleon [57]. However, the model does not account for the medium-range attraction [58, 59].

To describe the medium- and long-range behavior of nuclear forces, the hybrid quark model was developed by incorporating the exchanges of both π -meson and σ -meson at the baryon level [60]. The effective meson exchange potential between two nucleons was introduced to simulate the effects of the meson cloud surrounding the quark core. For consistency, the implementation of chiral symmetry at the quark potential level was essential [61]. The constituent quark mass arises from the spontaneous breaking of chiral symmetry at a certain momentum scale. Once this constituent quark mass is generated, the quarks must interact via Goldstone bosons. The π -meson and σ -meson exchanges at the quark level were incorporated in the non-relativistic quark model, called SU(2) ChQM. This model provides a satisfactory description of hadron spectra, nucleon-nucleon phase shifts, and the deuteron [62–64].

Later, the SU(3) ChQM was developed to investigate interactions between nucleons and hyperons, as well as hyperon-hyperon interactions [65]. In the model, the chiral symmetry is spontaneously broken in the light sector (u , d , and s) while it is explicitly broken in the heavy sector (b and c). The interactions mediated by the π -, K -, η -, and σ -meson exchange occur exclusively in the light quark sector.

It is a logical advancement to extend this model to encompass a broader range of hadron-hadron interactions, including those involving heavy hadrons. We employed the model to investigate single-flavored dibaryon bound states in the 1S_0 configuration [20]. Our findings were compared with results from various theoretical frameworks, particularly lattice QCD. Many of our conclusions were consistent and occasionally qualitatively aligned with those derived from other approaches. Furthermore, the model effectively describes the characteristics of the deuteron-like DD^* molecular state $T_{cc}^+(3875)$ [38]. These results indicate that our model is robust and physically valid in its representation of hadron-hadron interactions.

To sum up, the complete model Hamiltonian involved in this study is expressed as

$$\begin{aligned}
H_n &= \sum_{i=1}^n \left(m_i + \frac{\mathbf{p}_i^2}{2m_i} \right) - T_{\text{cm}} + \sum_{i<j}^n V_{ij}^{\text{oge}} + V_{ij}^{\text{con}} + V_{ij}^{\text{obe}} + V_{ij}^{\sigma}, \\
V_{ij}^{\text{oge}} &= \frac{\alpha_s}{4} \boldsymbol{\lambda}_i \cdot \boldsymbol{\lambda}_j \left(\frac{1}{r_{ij}} - \frac{\boldsymbol{\sigma}_i \cdot \boldsymbol{\sigma}_j}{6m_i m_j r_0^2(\mu_{ij}) r_{ij}} \right) e^{-\frac{r_{ij}}{r_0(\mu_{ij})}}, \quad V_{ij}^{\text{con}} = -a_c \boldsymbol{\lambda}_i \cdot \boldsymbol{\lambda}_j r_{ij}^2, \\
V_{ij}^{\text{obe}} &= V_{ij}^{\pi} \sum_{k=1}^3 \boldsymbol{\lambda}_i^k \cdot \boldsymbol{\lambda}_j^k + V_{ij}^K \sum_{k=4}^7 \boldsymbol{\lambda}_i^k \cdot \boldsymbol{\lambda}_j^k + V_{ij}^{\eta} (\boldsymbol{\lambda}_i^8 \cdot \boldsymbol{\lambda}_j^8 \cos \theta_P - \sin \theta_P) \\
V_{ij}^{\chi} &= \frac{g_{ch}^2}{4\pi} \frac{m_{\chi}^3}{12m_i m_j} \frac{\Lambda_{\chi}^2}{\Lambda_{\chi}^2 - m_{\chi}^2} \boldsymbol{\sigma}_i \cdot \boldsymbol{\sigma}_j \left(Y(m_{\chi} r_{ij}) - \frac{\Lambda_{\chi}^3}{m_{\chi}^3} Y(\Lambda_{\chi} r_{ij}) \right), \quad Y(x) = \frac{e^{-x}}{x}, \\
V_{ij}^{\sigma} &= -\frac{g_{ch}^2}{4\pi} \frac{\Lambda_{\sigma}^2 m_{\sigma}}{\Lambda_{\sigma}^2 - m_{\sigma}^2} \left(Y(m_{\sigma} r_{ij}) - \frac{\Lambda_{\sigma}}{m_{\sigma}} Y(\Lambda_{\sigma} r_{ij}) \right).
\end{aligned} \tag{1}$$

m_i and \mathbf{p}_i represent the mass and momentum of the quark q_i , respectively. T_{cm} denotes the center-of-mass kinetic energy. $\boldsymbol{\lambda}_i$ and $\boldsymbol{\sigma}_i$ stand for the SU(3) Gell-Mann matrices and SU(2) Pauli matrices, respectively. r_{ij} is the distance between q_i and q_j and μ_{ij} is their reduced mass, with the relation $r_0(\mu_{ij}) = \frac{\tilde{r}_0}{\mu_{ij}}$. The quark-gluon coupling constant α_s adopts an effective scale-dependent form,

$$\alpha_s(\mu_{ij}) = \frac{\alpha_0}{\ln \frac{\mu_{ij}^2}{\Lambda_0^2}}. \tag{2}$$

The symbol χ represents π , K and η meson and their mass m_{χ} take the experimentally determined values, while the cutoff parameters Λ_{χ} and the mixing angles θ_P are adopted from Ref. [66]. The mass parameter m_{σ} can be derived from the PCAC relation $m_{\sigma}^2 \approx m_{\pi}^2 + 4m_{u,d}^2$ [67]. The chiral coupling constant g_{ch} can be calculated from the πNN coupling constant through the following expression,

$$\frac{g_{ch}^2}{4\pi} = \left(\frac{3}{5} \right)^2 \frac{g_{\pi NN}^2}{4\pi} \frac{m_{u,d}^2}{m_N^2}. \tag{3}$$

The following step is to incorporate ordinary baryons within the quark model in order to determine the adjustable model parameters with the MINUIT program. This program is widely used for fitting models to data, aiming to minimize an objective function and derive the best-fit parameter values along with their associated uncertainties [68]. We minimize the mean square error

$$\Delta = \sum_{i=1}^N \frac{(M_i - m_i)^2}{N}$$

to fit the mass spectrum and to determine the adjustable parameters and their errors in the MINUIT program. N is the total number of baryons. M_i is the experimental mass of the i th baryon and m_i is its predicted mass in the

model. This objective function quantifies the goodness of fit between the model and the observed data.

The central values of the adjustable parameters, along with the heavy ground state baryon spectrum, were detailed in Tables I and II of our previous work [20]. In the current study, we present the adjustable parameters along with their associated uncertainties in Table I. It is noteworthy that the quark masses $m_{u,d}$ and m_s are held fixed during fitting baryon spectrum. The masses $m_{u,d}$ are set to one-third of the nucleon mass, namely $m_{u,d} = 313$ MeV, while m_s is fixed at 500 MeV in this investigation.

TABLE I: Model parameters. Quark masses and Λ_0 unit in MeV, a_c unit in $\text{MeV} \cdot \text{fm}^{-2}$, r_0 unit in $\text{MeV} \cdot \text{fm}$ and α_0 is dimensionless.

Parameter	m_c	m_b	a_c
Value	1613.7 ± 0.6	4981.6 ± 0.7	45.6 ± 0.5
Parameter	α_0	Λ_0	r_0
Value	3.76 ± 0.02	21.9 ± 0.2	95.7 ± 1.1

Based on the model parameters and their uncertainties, we can calculate the errors of the baryon spectrum inducing by the parameter uncertainties. The model Hamiltonian can be regarded as a function of model parameters, $H = H(x_1, \dots, x_6)$. The variance of the model hamiltonian resulting from the parameter uncertainties δx_i can be written as

$$\delta H = \sum_{i=1}^6 \frac{\partial H(x_1, \dots, x_6)}{\partial x_i} \delta x_i, \tag{4}$$

where x_i and δx_i represent the i -th adjustable parameter and its uncertainty, respectively. The energy uncertainty introduced by the parameter uncertainties can be calcu-

TABLE II: Mass spectra of baryon ground states unit in MeV and mass rms radius of quark core unit in fm. PDG is the abbreviation of particle data group. The “×” denotes that the state does not exist in the experiment.

Baryon	$I(J^P)$	Mass	Rms	PDG
Λ_c	$0(\frac{1}{2}^+)$	2270.3 ± 10.6	0.44	2286.46 ± 0.14
Σ_c	$1(\frac{1}{2}^+)$	2462.9 ± 8.3	0.47	2452.9 ± 0.4
Σ_c^*	$1(\frac{3}{2}^+)$	2492.9 ± 8.3	0.48	2518.41 ± 0.22
Ξ_{cc}	$\frac{1}{2}(\frac{1}{2}^+)$	3635.8 ± 7.9	0.43	3621.6 ± 0.4
Ξ_{cc}^*	$\frac{1}{2}(\frac{3}{2}^+)$	3667.5 ± 7.5	0.44	×
Λ_b	$0(\frac{1}{2}^+)$	5606.6 ± 10.5	0.29	5619.57 ± 0.16
Σ_b	$1(\frac{1}{2}^+)$	5814.3 ± 8.2	0.31	5810.56 ± 0.25
Σ_b^*	$1(\frac{3}{2}^+)$	5825.6 ± 8.2	0.32	5830.32 ± 0.27
Ξ_{bb}	$\frac{1}{2}(\frac{1}{2}^+)$	10263.5 ± 7.5	0.29	×
Ξ_{bb}^*	$\frac{1}{2}(\frac{3}{2}^+)$	10276.7 ± 7.3	0.29	×

lated using the formula,

$$\delta E_B = \langle \Phi_{IJ}^B | \delta H | \Phi_{IJ}^B \rangle, \quad (5)$$

where Φ_{IJ}^B is the eigen vector for baryon obtained by solving Schrödinger equation. The energy of baryons related to this work and their energy uncertainty are presented in Table II, which ranges from 7 MeV to 10 MeV.

In addition, we calculate the mass root-mean-square (rms) radius of quark core of baryons using their eigenvectors. The mass rms radius was defined as [69, 70]

$$\langle \mathbf{r}^2 \rangle^{\frac{1}{2}} = \left(\sum_{i=1}^3 \frac{m_i \langle (\mathbf{r}_i - \mathbf{R}_{\text{cm}})^2 \rangle}{m_1 + m_2 + m_3} \right)^{\frac{1}{2}}. \quad (6)$$

The numerical results are presented in Table II, which are in good agreement with those from [69, 70]. While the mass rms radius is not directly observable, it is still a valuable quantity that provides insight into the size of baryons within the framework of the constituent quark model. Generally, the mass rms radius of the quark core is smaller than the physical radius of the baryons, as it does not account for the contributions of the meson cloud surrounding the valence quarks, which are excluded from the model calculations.

III. WAVE FUNCTIONS OF DIBARYONS

The wave function of the dibaryons with well-defined isospin and spin (I and J) can be expressed as

$$\Psi_{IJ}^{\text{Dibaryon}} = \sum_{\xi} c_{\xi} \mathcal{A} \left\{ \left[\Phi_{I_1 J_1}^{B_1} \Phi_{I_2 J_2}^{B_2} \right]_{IJ} \phi_{lm}(\boldsymbol{\rho}) \right\}, \quad (7)$$

where $\Phi_{I_1 J_1}^{B_1}$ and $\Phi_{I_2 J_2}^{B_2}$ stand for the wave functions of the ground state baryons B_1 and B_2 , respectively. More details about the construction of baryons can be found in our previous work [20]. The square brackets indicate the Clebsch-Gordan couplings of spin and isospin. The summation index ξ encompasses all possible isospin-spin intermediate configurations $\{I_1, I_2, J_1, J_2\}$ that can be coupled to yield the total isospin I and angular momentum J of the dibaryons. The coefficients c_{ξ} are dictated by the dynamics of the model and the inherent properties of the baryons. They can be obtained by solving the eigen problem.

The term $\phi_{lm}(\boldsymbol{\rho})$ is the relative motion wave function between two baryons, where

$$\boldsymbol{\rho} = \frac{m_1 \mathbf{r}_1 + m_2 \mathbf{r}_2 + m_3 \mathbf{r}_3}{m_1 + m_2 + m_3} - \frac{m_4 \mathbf{r}_4 + m_5 \mathbf{r}_5 + m_6 \mathbf{r}_6}{m_4 + m_5 + m_6}. \quad (8)$$

Accurate numerical calculations are crucial for fully understanding the properties of dibaryons. The Gaussian Expansion Method (GEM) has demonstrated considerable efficacy in addressing the few-body problem within nuclear physics [71]. A recent comparative study highlighted the advantages of the GEM over both the resonating group method and the diffusion Monte Carlo method when it comes to investigating tetraquark bound states in quark models [72]. In this study, we employ the GEM to explore the properties of dibaryon states, thereby ensuring that our numerical results are both accurate and reliable. Within the GEM framework, the relative motion wave function $\phi_{lm}(\boldsymbol{\rho})$ can be expanded as a superposition of Gaussian functions with different widths, expressed as,

$$\phi_{lm}(\boldsymbol{\rho}) = \sum_{n=1}^{n_{\text{max}}} c_n N_{nl} x^l e^{-\nu_n x^2} Y_{lm}(\hat{\boldsymbol{\rho}}). \quad (9)$$

For further details on the GEM, refer to Ref. [71].

Note that a restriction must be imposed on the quantum numbers $\{I_1, I_2, J_1, J_2, I, J, l\}$ when the baryons B_1 and B_2 are identical particles in order to satisfy Fermi-Dirac statistics. Their quantum numbers must satisfy the relation $J_1 + J_2 - J + I_1 + I_2 - I + l = \text{odd}$. We primarily focus on the ground state of dibaryons, i.e., with $l = 0$, as these states are more likely to form bound states.

The present work mainly focus on the di- Ξ_{cc} and di- Ξ_{bb} states, uniformly denoted as $B_1(Q_1 Q_2 q_3) B_2(Q_4 Q_5 q_6)$, where Q_i stands for heavy charm and bottom quarks and q_i represents up and down quarks. \mathcal{A} is antisymmetrization operator acting on the identical quarks and can be expressed as

$$\mathcal{A} = \mathcal{A}_{1245} \mathcal{A}_{36}, \quad \mathcal{A}_{36} = (1 - P_{36}), \quad (10)$$

$$\mathcal{A}_{1245} = (1 - P_{14} - P_{15} - P_{24} - P_{25} + P_{14} P_{25}),$$

where P_{ij} is a permutation operator acting on the identical quarks i and j .

IV. NUMERICAL RESULTS AND DISCUSSIONS

A. Methodology

Next, we turn our attention to the investigation of the dibaryons within the quark models. By approximately exact solving the six-body Schrödinger equation

$$(H_6 - E_6)\Psi_{IJ}^{\text{Dibaryon}} = 0 \quad (11)$$

for the bound state problem with the Rayleigh-Ritz variational principle, we can achieve the eigenvalues and corresponding eigenvectors of the dibaryons.

The binding energy of the dibaryons can be calculated through the formula,

$$\Delta E_6 = E_6(\rho) - E_6(\infty). \quad (12)$$

$E_6(\rho)$ is the minimum energy of the dibaryons at the optimal inter-baryon separation ρ . $E_6(\infty)$ is the sum of the energies, $E(\infty) = E_{B_1} + E_{B_2}$, of two isolated ground state baryons in the quark model, i.e. the theoretical threshold of the dibaryons. If $\Delta E_6 \geq 0$, the dibaryon is unbound and can decay into two constituent baryons B_1 and B_2 via strong interactions. However, if $\Delta E_6 < 0$, the strong decay into two constituent baryons is forbidden, and the decay can only occur via weak or electromagnetic interactions. The binding energies of the dibaryon $\text{di-}\Xi_{cc}$ and $\text{di-}\Xi_{bb}$ with various isospin-spin configurations are presented in Tables III-VI in the following subsections. To provide a clearer and more intuitive representation of the binding energy, the energies of these dibaryon states and their corresponding thresholds are displayed in Figs. 1 and 2. The thresholds for the dibaryons with various isospin-spin configurations are indicated by dotted horizontal lines. This visualization offers a better understanding of the relative binding energies and the positioning of each state in relation to the respective thresholds.

The uncertainty of binding energy resulting from the parameter uncertainty can be written as

$$\delta(\Delta E_6) = \delta E_6 - \delta E_{B_1} - \delta E_{B_2}. \quad (13)$$

Because the same model parameters contribute to both the dibaryon and its corresponding baryon masses, the uncertainties arising from these parameters are strongly correlated. Consequently, when the dibaryon binding energy is calculated as their difference, these correlated contributions partially cancel, resulting in a reduced overall uncertainty, as illustrated in Tables III-VI. Importantly, these uncertainties reflect the statistical propagation from the model parameters, rather than an artificial suppression of errors. As a result, this subtraction of binding energy significantly reduces the influence of uncertainties in the model parameters and baryon spectra on the calculated binding energies. Comprehensive error

analysis indicate that the predicted dibaryon states are quantitatively reliable in the quark model.

To clarify the binding mechanism of the bound states, we analyze the contributions from various interactions to the binding energy ΔE_6 using its eigenvector,

$$\begin{aligned} \Delta\langle V^\chi \rangle &= \langle \Psi_{IJ}^{\text{Dibaryon}} | V^\chi | \Psi_{IJ}^{\text{Dibaryon}} \rangle - \langle \Phi_{I_1 J_1}^{B_1} | V^\chi | \Phi_{I_1 J_1}^{B_1} \rangle \\ &\quad - \langle \Phi_{I_2 J_2}^{B_2} | V^\chi | \Phi_{I_2 J_2}^{B_2} \rangle, \end{aligned} \quad (14)$$

where χ represents all types of interactions in the quark models. Similarly, we can also obtain the kinetic contribution to the binding energy. Additionally, we compute the distances between two baryons in the bound state,

$$\langle \rho^2 \rangle^{\frac{1}{2}} = \langle \Psi_{IJ}^{\text{Dibaryon}} | \rho^2 | \Psi_{IJ}^{\text{Dibaryon}} \rangle^{\frac{1}{2}}. \quad (15)$$

The numerical results from these calculations are presented in Tables III and V. Comparing with the sizes of single baryons, one can intuitively figure out the spatial configuration of the bound state. If $\langle \rho^2 \rangle^{\frac{1}{2}}$ is obviously greater than the sum of the sizes of the two baryons, the baryons are considered to be completely separated, forming a loose, deuteron-like configuration. Otherwise, the dibaryon is a compact hexaquark state.

B. $\text{Di-}\Xi_{cc}$ states

The dibaryon $\text{di-}\Xi_{cc}$ with $0(1^+)$ has three possible configurations: $\Xi_{cc}\Xi_{cc}$, $\Xi_{cc}\Xi_{cc}^*$, and $\Xi_{cc}^*\Xi_{cc}^*$. From Table III and Fig. 1, it can be observed that $\Xi_{cc}\Xi_{cc}$ with $0(1^+)$ can not produce a bound state in the quark model because of the lack of binding force. In contrast, this dibaryon configuration shows a binding energy of approximately 0.7 MeV and a root-mean-square radius of 3.23 fm when using a reasonable cutoff of 1.1 GeV in the OBE model [16]. This suggests that the $\Xi_{cc}\Xi_{cc}$ with $0(1^+)$ is a promising candidate for a deuteron-like molecular state in the OBE model.

The distance between two baryons in the $\Xi_{cc}\Xi_{cc}$ with $0(1^+)$ is exceptionally large, potentially approaching infinity, which serves as a means to mitigate the repulsive interactions. Consequently, the contributions from various interactions, as well as the kinetic energy associated with the system, effectively diminish to nearly zero due to the large spatial separation.

The dynamical calculation involved in this work contrasts with the Born-Oppenheimer approximation employed in molecular physics, where nuclei are assumed to be static because of their larger masses than electrons. Similar to the Born-Oppenheimer approximation, we present the effective potential between two baryons at specific fixed distances, as illustrated in Table IV. It is evident that the kinetic term plays a significant role in inhibiting the formation of the bound state $\Xi_{cc}\Xi_{cc}$ with $0(1^+)$, which is also hold truth for other unbound dibaryon states.

Both $\Xi_{cc}\Xi_{cc}^*$ and $\Xi_{cc}^*\Xi_{cc}^*$ with $0(1^+)$ have the potential

TABLE III: The binding energy ΔE_6 of the di- Ξ_{cc} state and the contribution of each part in the Hamiltonian to ΔE_6 , ΔV^{con} , ΔV^{coul} , ΔV^{cm} , ΔT , ΔV^σ , ΔV^π , and ΔV^η are confinement term, Coulomb term, chromomagnetic term, kinetic energy, σ -, π -, and η -meson exchange term, respectively, unit in MeV. $\langle r^2 \rangle^{\frac{1}{2}}$ represents the average size of a baryon and $\langle \rho^2 \rangle^{\frac{1}{2}}$ is the distance between two baryons, unit in fm.

$I(J^P)$	Dibaryon	ΔE_6	ΔV^{con}	ΔV^{coul}	ΔV^{cm}	ΔT	ΔV^π	ΔV^η	ΔV^σ	$\langle r^2 \rangle^{\frac{1}{2}}$	$\langle \rho^2 \rangle^{\frac{1}{2}}$
0(1 ⁺)	$\Xi_{cc}\Xi_{cc}$	Unbound								0.44	$\rightarrow \infty$
	$\Xi_{cc}\Xi_{cc}^*$	-1.5 ± 0.2	-1.4	-1.5	-1.8	10.0	-2.2	0.1	-4.7	0.44	2.37
	$\Xi_{cc}^*\Xi_{cc}^*$	-3.3 ± 0.2	-1.1	-1.5	-1.4	3.6	3.0	-0.3	-5.6	0.44	1.87
	Coupling	-7.1 ± 0.1	-2.1	-2.1	-2.2	3.9	3.7	-0.3	-8.0	0.44	1.40

TABLE IV: Effective potential of the state $\Xi_{cc}\Xi_{cc}$ with 0(1⁺) when the distance $\langle \rho^2 \rangle^{\frac{1}{2}}$ ranges from 0.50 fm to 3.00 fm, see the caption for Table III.

$I(J^P)$	Dibaryon	ΔE_6	ΔV^{con}	ΔV^{coul}	ΔV^{cm}	ΔT	ΔV^π	ΔV^η	ΔV^σ	$\langle r^2 \rangle^{\frac{1}{2}}$	$\langle \rho^2 \rangle^{\frac{1}{2}}$
0(1 ⁺)	$\Xi_{cc}\Xi_{cc}$	106.8 ± 0.2	-17.5	25.0	2.9	90.5	-16.3	1.6	-13.8	0.44	0.50
		53.3 ± 0.1	-1.1	-6.8	-2.4	74.6	-1.2	0.1	-10.0	0.44	1.00
		27.3 ± 0.1	-2.4	-6.7	-2.0	45.1	0.7	-0.1	-7.3	0.44	1.50
		17.7 ± 0.1	-2.0	-5.1	-1.6	31.3	0.8	-0.1	-5.7	0.44	2.00
		13.1 ± 0.1	-1.6	-3.9	-1.3	23.8	0.8	-0.1	-4.8	0.44	2.50
		9.6 ± 0.1	-1.2	-2.9	-1.0	17.8	0.7	-0.1	-3.9	0.44	3.00

to form shallow bound states, with binding energies of approximately 1.5 MeV and 3.3 MeV, respectively, relative to their constituent particles in the quark model. In the OBE model, the $\Xi_{cc}\Xi_{cc}^*$ 0(1⁺) forms a shallow bound state, with a binding energy ranging from 4.7 MeV to 12.6 MeV, depending on the cutoff parameter Λ , which varies between 1.2 GeV and 1.6 GeV [17]. In contrast, the $\Xi_{cc}^*\Xi_{cc}^*$ with 0(1⁺) leads to a deep bound state, with binding energies ranging from 25.3 MeV to 39.8 MeV when the cutoff parameter Λ is between 0.82 GeV and 0.84 GeV [17].

In the formation of the bound states $\Xi_{cc}\Xi_{cc}^*$ and $\Xi_{cc}^*\Xi_{cc}^*$ with 0(1⁺) in the quark model, all the interactions V^{con} , V^{coul} , V^{cm} , and V^σ contribute a little attractive force, with V^σ playing the dominant role, as shown in Table III. In contrast, the π -meson exchange is repulsive in the $\Xi_{cc}\Xi_{cc}^*$ with 0(1⁺), while it is attractive in the $\Xi_{cc}^*\Xi_{cc}^*$ with 0(1⁺). Comparatively speaking, the η -meson exchange is very small and can almost be considered negligible. Overall contributions from those three meson exchanges is attractive. Our numerical results indicate that once those three meson exchanges, which just occurs between two subclusters and do not affect the corresponding threshold, are excluded from the quark model, those two bound states disappear. This indicated that the meson exchange force plays a pivotal role in the formation of the bound states. The main factor hindering the formation of the $\Xi_{cc}^{(*)}$ and Ξ_{cc}^* subclusters into the bound dibaryon is the relative kinetic energy between two sub-

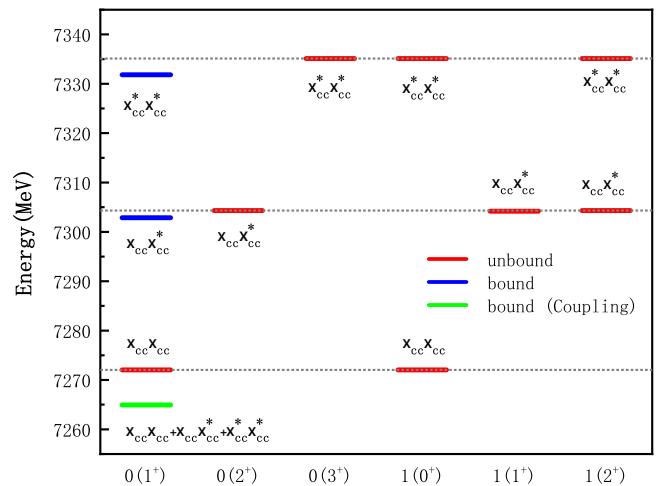


FIG. 1: The energy spectrum of the di- Ξ_{cc} system. The thresholds, $\Xi_{cc}\Xi_{cc}$, $\Xi_{cc}\Xi_{cc}^*$, and $\Xi_{cc}^*\Xi_{cc}^*$, are marked by three dotted horizontal lines, arranged from bottom to top.

clusters.

It is important to highlight that this processing method concerning meson exchange interactions, specifically, evaluating its contribution by suppressing the meson exchange interaction, is applicable only to dibaryon systems in which each baryon consists of two heavy quarks and one light quark. Examples of such systems include $\Xi_{cc}^{(*)}\Xi_{cc}^{(*)}$ and $\Xi_{bb}^{(*)}\Xi_{bb}^{(*)}$. However, this processing method

is not valid for other dibaryon systems that involve multiple light quarks, such as $\Lambda_c\Lambda_c$ and $\Lambda_b\Lambda_b$, as the masses of the individual hadrons would be altered when the meson exchange interaction is turned off in the analysis of the interactions between two baryons.

The average distance $\langle\rho^2\rangle^{\frac{1}{2}}$ between Ξ_{cc} (Ξ_{cc}^*) and Ξ_{cc}^* is 2.37 (1.87) fm, as shown in Table III, which is significantly larger than twice the size, approximately 0.44 fm of the single Ξ_{cc}^* baryon, as indicated in Table II. This suggests that two baryons are well separated and do not completely overlap, implying that both $\Xi_{cc}\Xi_{cc}^*$ and $\Xi_{cc}^*\Xi_{cc}^*$ with $0(1^+)$ resemble a deuteron-like dibaryon in the quark model. In the OBE model, the $\Xi_{cc}\Xi_{cc}^*$ with $0(1^+)$ behaves as a deuteron-like dibaryon, as its root-mean-square radius lies between 1.17 fm and 2.15 fm. However, the $\Xi_{cc}^*\Xi_{cc}^*$ with $0(1^+)$ may not be an ideal candidate for a molecular state, as its root-mean-square radius is less than 1.0 fm [17].

From a quantum mechanical standpoint, the dibaryon states should be the linear combinations of all possible isospin-spin configurations. The mixing of these configurations serves to push down the energy of the states. Upon coupling the $\Xi_{cc}\Xi_{cc}$, $\Xi_{cc}\Xi_{cc}^*$, and $\Xi_{cc}^*\Xi_{cc}^*$ with $0(1^+)$, the final energy of the di- Ξ_{cc} system with $0(1^+)$ is approximately -7.1 MeV relative to the threshold $\Xi_{cc}\Xi_{cc}$. The coupled channel effect enhances the attraction between two subclusters, especially for the σ meson exchange, as shown in Table III. Despite this, the di- Ξ_{cc} system with $0(1^+)$ maintains a deuteronlike configuration, with the distance between the two subclusters being approximately 1.40 fm. Its main component is $\Xi_{cc}\Xi_{cc}$, accounting for over 99%, while the contributions from $\Xi_{cc}\Xi_{cc}^*$ and $\Xi_{cc}^*\Xi_{cc}^*$ are less than 1%. The coupled channel effect plays a vital role in the formation of the di- Ξ_{cc} bound system with $0(1^+)$.

The coupled channel effect, incorporating not only S-wave but also D-wave components, in the di- Ξ_{cc} system with $0(1^+)$ was considered in the OBE model [17]. This system is a deep bound state with a binding energy ranging from 36.5 MeV to 49.3 MeV relative to the threshold $\Xi_{cc}\Xi_{cc}$, and its size is approximately 1 fm. The S-wave components dominate the di- Ξ_{cc} system, while the D-wave components are exceedingly small.

Other isospin-spin configurations, such as $\Xi_{cc}\Xi_{cc}^*$ with $0(2^+)$, $\Xi_{cc}^*\Xi_{cc}^*$ with $0(3^+)$, $\Xi_{cc}\Xi_{cc}$ and $\Xi_{cc}^*\Xi_{cc}^*$ with $1(0^+)$, $\Xi_{cc}\Xi_{cc}^*$ with $1(1^+)$, and $\Xi_{cc}\Xi_{cc}^*$ and $\Xi_{cc}^*\Xi_{cc}^*$ with $0(2^+)$ do not form any bound states in the quark model, even when considering the coupled channel effects in the calculations, as shown in Table III and Fig. 1. In the OBE model, the $\Xi_{cc}^*\Xi_{cc}^*$ with $1(2^+)$ is fail to form a bound state [17]. In stark contrast, the remaining isospin-spin configurations are good candidates of deuteronlike molecular states [17]. On the whole, the OBE model can provide more attractive forces than the quark model in the di- Ξ_{cc} system.

C. Di- Ξ_{bb} states

The di- Ξ_{bb} system exhibits the same isospin-spin configurations as the di- Ξ_{cc} system. In accordance with the heavy quark flavor symmetry, the properties of the di- Ξ_{bb} system should be analogous to those of the di- Ξ_{cc} system. However, the significantly larger mass of Ξ_{bb}^* can reduce the relative kinetic between Ξ_{bb}^* and Ξ_{bb}^* , allowing them to approach each other more closely. As a result, the interactions between Ξ_{bb}^* and Ξ_{bb}^* should become stronger. In general, this makes the di- Ξ_{bb} system more prone to form a bound state compared to the di- Ξ_{cc} system.

From Table V and Fig. 2, it can be observed that all the $\Xi_{bb}\Xi_{bb}$, $\Xi_{bb}\Xi_{bb}^*$, and $\Xi_{bb}^*\Xi_{bb}^*$ with $0(1^+)$ are capable of forming deuteronlike bound states within the quark model. Their corresponding binding energies are -6.1 MeV, -14.3 MeV, and -13.7 MeV, respectively, relative to the energy of their constituent particles. The distances between Ξ_{bb}^* and Ξ_{bb}^* are approximately 1 fm. However, despite this small distance, their spatial configuration does not form a compact hexaquark. Instead, they resemble a loosely bound deuteron-like molecule, due to the small size of the Ξ_{bb}^* baryons.

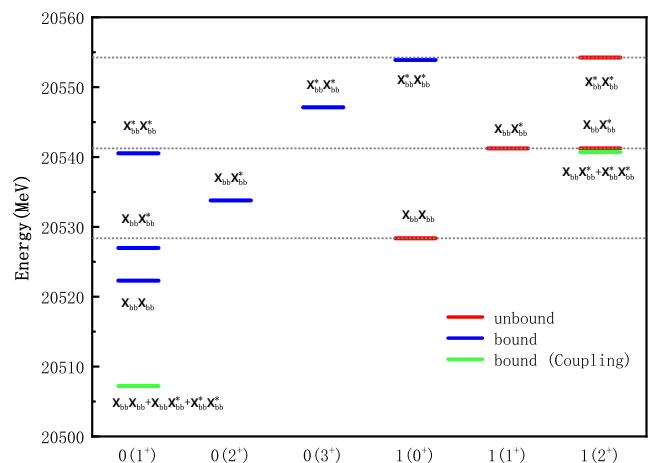


FIG. 2: The energy spectrum of the di- Ξ_{bb} systems. The thresholds, $\Xi_{bb}\Xi_{bb}$, $\Xi_{bb}\Xi_{bb}^*$, and $\Xi_{bb}^*\Xi_{bb}^*$, are marked by three dotted horizontal lines, arranged from bottom to top.

Similar to the di- Ξ_{cc} system, all the interactions V^{con} , V^{coul} , V^{cm} , and V^σ contribute a few attractive force, with V^σ playing the dominant role, as shown in Table V. However, the proportion of the overall contributions from those meson exchanges to the binding energy is significantly reduced. If we turn off those meson exchanges in the quark model, the $\Xi_{bb}\Xi_{bb}$ and $\Xi_{bb}\Xi_{bb}^*$ with $0(1^+)$ can still form deuteronlike bound states with a binding energy of several MeVs, as shown in Table VI. This demonstrates that the meson exchange forces are secondary in the formation of those two bound states. However, the

TABLE V: The binding energy ΔE_6 of di- Ξ_{bb} state, see the caption for Table III.

$I(J^P)$	Dibaryon	ΔE_6	ΔV^{con}	ΔV^{coul}	ΔV^{cm}	ΔT	ΔV^π	ΔV^η	ΔV^σ	$\langle r^2 \rangle^{\frac{1}{2}}$	$\langle \rho^2 \rangle^{\frac{1}{2}}$
0(1 ⁺)	$\Xi_{bb}\Xi_{bb}$	-6.1 ± 0.2	-1.5	-5.4	-2.5	7.8	2.8	-0.3	-7.0	0.29	1.03
	$\Xi_{bb}\Xi_{bb}^*$	-14.3 ± 0.1	-3.7	-10.0	-4.4	9.1	7.1	-0.7	-11.6	0.29	0.90
	$\Xi_{bb}^*\Xi_{bb}^*$	-13.7 ± 0.1	-6.2	-8.3	-7.7	28.4	-7.9	0.5	-12.6	0.29	0.81
	Coupling	-21.2 ± 0.2	-10.5	-9.0	-11.1	80.5	-60.6	6.5	-17.0	0.29	0.53
0(2 ⁺)	$\Xi_{bb}\Xi_{bb}^*$	-7.4 ± 0.2	-1.0	-5.6	-1.4	0.8	7.2	-0.5	-7.0	0.29	1.30
0(3 ⁺)	$\Xi_{bb}^*\Xi_{bb}^*$	-7.1 ± 0.2	-0.9	-5.2	-1.1	0.5	6.9	-0.5	-6.7	0.29	1.35
1(0 ⁺)	$\Xi_{bb}\Xi_{bb}$	Unbound								0.29	$\rightarrow \infty$
	$\Xi_{bb}^*\Xi_{bb}^*$	-0.3 ± 0.1	0.1	-0.1	1.1	-1.0	1.4	0.3	-2.2	0.29	3.36
	Coupling	Unbound								0.29	$\rightarrow \infty$
1(1 ⁺)	$\Xi_{bb}\Xi_{bb}^*$	Unbound								0.29	$\rightarrow \infty$
1(2 ⁺)	$\Xi_{bb}\Xi_{bb}^*$	Unbound								0.29	$\rightarrow \infty$
	$\Xi_{bb}^*\Xi_{bb}^*$	Unbound								0.29	$\rightarrow \infty$
	Coupling	-0.5 ± 0.1	0.1	-0.1	1.6	-1.7	1.6	0.2	-2.2	0.29	2.79

TABLE VI: The binding energy ΔE_6 of di- Ξ_{bb} state in the model without meson exchanges, see the caption for Table III.

$I(J^P)$	Dibaryon	ΔE_6	ΔV^{con}	ΔV^{coul}	ΔV^{cm}	ΔT	ΔV^π	ΔV^η	ΔV^σ	$\langle r^2 \rangle^{\frac{1}{2}}$	$\langle \rho^2 \rangle^{\frac{1}{2}}$
0(1 ⁺)	$\Xi_{bb}\Xi_{bb}$	-2.2 ± 0.1	-0.2	-2.6	-1.7	2.3				0.29	1.63
	$\Xi_{bb}\Xi_{bb}^*$	-9.1 ± 0.1	-2.3	-7.4	-4.0	4.7				0.29	0.97
	$\Xi_{bb}^*\Xi_{bb}^*$	Unbound								0.29	$\rightarrow \infty$
	Coupling	-6.7 ± 0.1	-1.0	-7.3	8.3	-6.7				0.29	0.93
0(2 ⁺)	$\Xi_{bb}\Xi_{bb}^*$	-7.2 ± 0.1	-1.4	-7.2	-1.6	2.9				0.29	1.25
0(3 ⁺)	$\Xi_{bb}^*\Xi_{bb}^*$	-6.8 ± 0.1	-1.4	-6.6	-1.2	2.3				0.29	1.29
1(2 ⁺)	$\Xi_{bb}\Xi_{bb}^*$	Unbound								0.29	$\rightarrow \infty$
	$\Xi_{bb}^*\Xi_{bb}^*$	Unbound								0.29	$\rightarrow \infty$
	Coupling	-0.3 ± 0.1	0.1	-0.7	2.1	-1.8				0.29	3.18

$\Xi_{bb}^*\Xi_{bb}^*$ with 0(1⁺) cannot yield a bound state when turning off those meson exchanges in the quark model. This suggests that the meson exchanges play a critical role in the formation of bound state $\Xi_{bb}^*\Xi_{bb}^*$ with 0(1⁺).

After coupling of the $\Xi_{bb}\Xi_{bb}$, $\Xi_{bb}\Xi_{bb}^*$, and $\Xi_{bb}^*\Xi_{bb}^*$ with 0(1⁺), the final binding energy is -21.2 MeV relative to the threshold $\Xi_{bb}\Xi_{bb}$ in the quark model, as illustrated in Table V and Fig. 2. This bound state is a compact hexaquark state because two baryons are partly overlapped, which is evidenced by the sizes of baryons $\Xi_{bb}^{(*)}$ and the distance between two baryons. The probabilities of the $\Xi_{bb}\Xi_{bb}$, $\Xi_{bb}\Xi_{bb}^*$, and $\Xi_{bb}^*\Xi_{bb}^*$ components are 41%, 42% and 17%, respectively, in this compact hexaquark state. The binding force of this compact state primarily arises from the meson exchanges, particularly the π -meson ex-

change, as shown in Table V. Therefore, the di- Ξ_{bb} with 0(1⁺) can only form a shallow bound state with a binding energy of approximately -6.7 MeV, when even considering the coupled channel effect $\Xi_{bb}\Xi_{bb}$, $\Xi_{bb}\Xi_{bb}^*$, and $\Xi_{bb}^*\Xi_{bb}^*$ in the quark model, excluding the meson exchanges, as shown in Table VI.

Both $\Xi_{bb}\Xi_{bb}^*$ with 0(2⁺) and $\Xi_{bb}^*\Xi_{bb}^*$ with 0(3⁺) can form a deuteronlike bound state with a binding energy of around -7.0 MeV and a size of approximately 1.30 fm, whether or not the meson exchanges are involved in the quark model, as illustrated in Tables V and VI. This result arises because the contributions from the π and σ meson exchanges nearly cancel each other out, while the contribution from the η meson exchange is negligible.

The $\Xi_{bb}\Xi_{bb}$ with 1(0⁺) is unbound in the quark model,

as shown in Table V and Fig. 2. However, the $\Xi_{bb}^* \Xi_{bb}^*$ with $1(0^+)$ can form a deuteronlike bound state, with a binding energy of -0.3 MeV relative to the threshold $\Xi_{bb}^* \Xi_{bb}^*$. Its dominant binding force arises from the σ meson exchange. If the meson exchanges are excluded from the quark model, this bound state ceases to exist. Additionally, the kinetic energy also contributes a slight attraction, approximately -1.0 MeV. The reduction in the kinetic energy arises from the negative exchange kinetic term [73], which is referred to as the hadron covalent bond [20]. The coupled channel effect between $\Xi_{bb} \Xi_{bb}$ and $\Xi_{bb}^* \Xi_{bb}^*$ does not push down the energy of the $\Xi_{bb} \Xi_{bb}$ with $1(0^+)$ below its threshold.

The $\Xi_{bb} \Xi_{bb}^*$ with $1(1^+)$, $\Xi_{bb} \Xi_{bb}^*$ and $\Xi_{bb}^* \Xi_{bb}^*$ with $1(2^+)$ can not form any bound states relative to their corresponding threshold in the quark model. After coupling $\Xi_{bb} \Xi_{bb}^*$ and $\Xi_{bb}^* \Xi_{bb}^*$ with $1(2^+)$, this system can establish a deuteronlike bound state with a binding energy of approximately -0.5 MeV and a large size of 2.79 fm. The dominant component of this bound state is $\Xi_{bb} \Xi_{bb}^*$, contributing 98%, while the $\Xi_{bb}^* \Xi_{bb}^*$ component is minimal, making up only 2%. In this bound state, the meson exchanges only contribute a little attraction of -0.4 MeV, as shown in Table V. This bound state persists even when switching off the meson exchanges. This suggests that the primary mechanism for the binding is not the meson exchanges, but rather the reduction in the kinetic energy, i.e. the so-called hadron covalent bond [20].

V. SUMMARY

Inspired by the $T_{cc}^+(3875)$ signal discovered by the LHCb Collaboration, we systematically examine the properties of the heavy dibaryons di- Ξ_{cc} and di- Ξ_{bb} across various isospin-spin configurations in the nonrelativistic quark model. In the calculation, we employ the Gaussian expansion method, a high-precision numerical method, to solve the six-body Schrödinger equations exactly. We analyze their binding energies and spatial structures. By decomposing the attractions from various sources, we explore the dynamical effects that govern the formation of stable bound states under strong interactions.

The $\Xi_{cc} \Xi_{cc}$ with $0(1^+)$ can not form a bound state in the quark model. Both $\Xi_{cc} \Xi_{cc}^*$ and $\Xi_{cc}^* \Xi_{cc}^*$ with $0(1^+)$ can form deuteronlike bound states, with binding energies of approximately -1.5 MeV and -3.3 MeV and sizes of 2.37 fm and 1.87 fm, respectively. The σ meson exchange plays a decisive role in their formation. The coupled channel effect of those three configurations with $0(1^+)$ enhances the attractions between two subclusters, especially for the σ meson exchange. The di- Ξ_{cc} system with $0(1^+)$ maintains a deuteronlike configuration, with the binding energy of -7.5 MeV and the size of approximately 1.40 fm. Its predominant component is $\Xi_{cc} \Xi_{cc}$, accounting for over 99%, while the contributions from $\Xi_{cc} \Xi_{cc}^*$ and $\Xi_{cc}^* \Xi_{cc}^*$ are less than 1%. Other isospin-spin configurations, such as $0(2^+)$, $0(3^+)$, $1(0^+)$, $1(1^+)$ and

$1(2^+)$, of the di- Ξ_{cc} system can not establish any bound states in the quark model.

The $\Xi_{bb} \Xi_{bb}$, $\Xi_{bb} \Xi_{bb}^*$ and $\Xi_{bb}^* \Xi_{bb}^*$ with $0(1^+)$ can establish a deuteronlike bound state, with binding energies of -6.1 MeV, -14.3 MeV and -13.7 MeV and sizes of 1.03 fm, 0.90 fm and 0.81 fm in the quark model, respectively. When these three configurations are coupled, the di- Ξ_{bb} system with $0(1^+)$ is a compact hexaquark state, with a binding energy of -21.2 MeV and a size of 0.53 fm. The probabilities of the $\Xi_{bb} \Xi_{bb}$, $\Xi_{bb} \Xi_{bb}^*$, and $\Xi_{bb}^* \Xi_{bb}^*$ components are approximately 41%, 42% and 17%, respectively, in this compact hexaquark state. The binding force of this compact state primarily arises from the meson exchanges, particularly the π -meson exchange.

Both $\Xi_{bb} \Xi_{bb}^*$ with $0(2^+)$ and $\Xi_{bb}^* \Xi_{bb}^*$ with $0(3^+)$ can form a deuteronlike bound state with a binding energy of around -7.0 MeV and a size of approximately 1.30 fm, whether or not the meson exchanges are involved in the quark model. The $\Xi_{bb} \Xi_{bb}$ with $1(0^+)$ is unbound while the $\Xi_{bb}^* \Xi_{bb}^*$ with $1(0^+)$ can form a deuteronlike bound state, with a binding energy of -0.3 MeV and a size of 3.36 fm. Its dominant binding force arises from the σ meson exchange. Additionally, the hadron covalent bond also contributes a slight attraction, approximately -1.0 MeV.

The $\Xi_{bb} \Xi_{bb}^*$ with $1(1^+)$, $\Xi_{bb} \Xi_{bb}^*$ and $\Xi_{bb}^* \Xi_{bb}^*$ with $1(2^+)$ can not form any bound states in the quark model. After coupling $\Xi_{bb} \Xi_{bb}^*$ and $\Xi_{bb}^* \Xi_{bb}^*$ with $1(2^+)$, this system can establish a deuteronlike bound state with a binding energy of approximately -0.5 MeV and a large size of 2.79 fm. The dominant component of this bound state is $\Xi_{bb} \Xi_{bb}^*$, contributing 98%, while the $\Xi_{bb}^* \Xi_{bb}^*$ component is minimal, making up only 2%. Its primary binding mechanism is not the meson exchanges, but rather the hadron covalent bond.

The information on the heavy dibaryon states presented in this work is expected to enhance our understanding of their properties and structures from a phenomenological perspective. We also advocate various theoretical frames to comprehensively explore the properties of those dibaryon states. Those works are attempted to contribute meaningfully to the hadron physics by bridging the gap between theoretical predictions and experimental realizations. As experimental facilities such as the LHCb and forthcoming high-luminosity colliders push the boundaries of hadron physics, the discovery of those dibaryon states may soon be attainable, despite the challenges associated with their production in experiments.

Acknowledgments

This research is supported by the National Natural Science Foundation of China under Grants No. 12305096, Chongqing Natural Science Foundation under Project No. CSTB2025NSCQ-GPX0516, and the Fundamental Research Funds for the Central Universities under Grant

-
- [1] H. De Vries, C.W. De Jager and C. De Vries, *Atom. Data Nucl. Data Tabl.* **36**, 495 (1987).
- [2] H. Clement, *Prog. Part. Nucl. Phys.* **93**, 195 (2017).
- [3] H. Clement and T. Skorodko, *Chin. Phys. C* **45**, 022001 (2021).
- [4] Y.B. Dong, P.N. Shen and Z.Y. Zhang, *Prog. Part. Nucl. Phys.* **131**, 104045 (2023).
- [5] A. Gal and H. Garcilazo, *Phys. Rev. Lett.* **111**, 172301 (2013).
- [6] A. Gal and H. Garcilazo, *Nucl. Phys. A* **928**, 73 (2014).
- [7] Y. Dong, A. Faessler and V.E. Lyubovitskij, *Prog. Part. Nucl. Phys.* **94**, 282 (2017).
- [8] F.K. Guo, C. Hanhart, U.G. Meißner, Q. Wang, Q. Zhao, and B.S. Zou, *Rev. Mod. Phys.* **90**, no.1, 015004 (2018) [erratum: *Rev. Mod. Phys.* **94**, 029901 (2022)].
- [9] X.K. Dong, F.K. Guo and B.S. Zou, *Commun. Theor. Phys.* **73**, 125201 (2021).
- [10] X.K. Dong, F.K. Guo and B.S. Zou, *Progr. Phys.* **41**, 65 (2021).
- [11] H.X. Chen, W.Chen, X.Liu, Y.R. Liu and S.L. Zhu, *Rept. Prog. Phys.* **86**, 026201 (2023).
- [12] L. Meng, B. Wang, G.J. Wang and S.L. Zhu, *Phys. Rept.* **1019**, 1 (2023).
- [13] H.X. Huang, C.R. Deng, X.J. Liu, Y. Tan and J.L. Ping, *Symmetry* **15**, 1298 (2023).
- [14] M.Z. Liu, Y.W. Pan, Z.W. Liu, T.W. Wu, J.X. Lu and L.S. Geng, *Phys. Rept.* **1108**, 1 (2025).
- [15] T.F. Carames and A. Valcarce, *Phys. Rev. D* **92**, 034015 (2015).
- [16] L. Meng, N. Li and S.L. Zhu, *Phys. Rev. D* **95**, 114019 (2017).
- [17] B. Yang, L. Meng and S.L. Zhu, *Eur. Phys. J. A* **56**, 67 (2020).
- [18] R. Chen, F.L. Wang, A. Hosaka and X. Liu, *Phys. Rev. D* **97**, 114011 (2018).
- [19] Z.G. Wang, *Phys. Rev. D* **102**, 034008 (2020).
- [20] C.R. Deng, *Phys. Rev. D* **108**, 054037 (2023).
- [21] B. Wang, K. Chen, L. Meng and S.L. Zhu, *Phys. Rev. D* **110**, 014038 (2024).
- [22] L. Zhang, T. Doi, Y. Lyu, T. Hatsuda and Y.G. Ma, *Phys. Lett. B* **871** 139998 (2025).
- [23] Y. Cui, Y.H. Wu, X.M. Zhu, H.X. Huang and J.L. Ping, *Phys. Rev. D* **111**, 114018 (2025).
- [24] P. Junnarkar and N. Mathur, *Phys. Rev. Lett.* **123**, 162003 (2019).
- [25] Y. Lyu, H. Tong, T. Sugiura, S. Aoki, T. Doi, T. Hatsuda, J. Meng and T. Miyamoto, *Phys. Rev. Lett.* **127**, 072003 (2021).
- [26] N. Mathur, M. Padmanath and D. Chakraborty, *Phys. Rev. Lett.* **130**, 111901 (2023).
- [27] P.M. Junnarkar and N. Mathur, *Phys. Rev. D* **111**, 014512 (2025).
- [28] H.Y. Xing, Y.Q. Geng, C. Liu, L.M. Liu, P. Sun, J.J. Wu, Z.C. Yan and R.L. Zhu, *Chin. Phys. C* **49**, 063107 (2025).
- [29] M.J. Savage and M.B. Wise, *Phys. Lett. B* **248**, 177 (1990).
- [30] M.Z. Liu, F.Z. Peng, M. Sánchez Sánchez and M.P. Valderrama, *Phys. Rev. D* **98**, 114030 (2018).
- [31] Y.W. Pan, M.Z. Liu, F.Z. Peng, M. Sánchez Sánchez, L.S. Geng and M. Pavon Valderrama, *Phys. Rev. D* **102**, 011504 (2020).
- [32] Y.W. Pan, M.Z. Liu and L.S. Geng, *Phys. Rev. D* **102**, 054025 (2020).
- [33] Y.W. Pan, T.W. Wu, M.Z. Liu and L.S. Geng, *Eur. Phys. J. C* **82**, 908 (2022).
- [34] R. Aaij *et al.* [LHCb], *Nature Phys.* **18**, 751 (2022).
- [35] R. Aaij *et al.* [LHCb], *Nature Commun.* **13**, 3351 (2022).
- [36] N. Mathur and M. Padmanath, *PoS LATTICE2021*, 443 (2022).
- [37] R. Chen, Q. Huang, X. Liu and S.L. Zhu, *Phys. Rev. D* **104**, 114042 (2021).
- [38] C.R. Deng and S.L. Zhu, *Phys. Rev. D* **105**, 054015 (2022).
- [39] M. Karliner and J.L. Rosner, *Phys. Rev. D* **105**, 034020 (2022).
- [40] M. Albaladejo, *Phys. Lett. B* **829**, 137052 (2022).
- [41] C.R. Deng and S.L. Zhu, *Sci. Bull.* **67**, 1522 (2022).
- [42] Y. Li, Y.B. He, X.H. Liu, B. Chen and H.W. Ke, *Eur. Phys. J. C* **83**, 258 (2023).
- [43] T. Aoki, S. Aoki and T. Inoue, *Phys. Rev. D* **108**, 054502 (2023).
- [44] C. Alexandrou, J. Finkenrath, T. Leontiou, S. Meinel, M. Pflaumer and M. Wagner, *Phys. Rev. Lett.* **132**, 151902 (2024).
- [45] M. Padmanath, A. Radhakrishnan and N. Mathur, *Phys. Rev. Lett.* **132**, 201902 (2024).
- [46] W.Y. Liu, H.X. Chen and E. Wang, *Phys. Rev. D* **107**, 054041 (2023).
- [47] Z.H. Lin, C.S. An and C.R. Deng, *Phys. Rev. D* **109**, 056005 (2024).
- [48] A. Radhakrishnan, M. Padmanath and N. Mathur, *Phys. Rev. D* **110**, 034506 (2024).
- [49] X. Chen and L. Ma, *Eur. Phys. J. A* **61**, 150 (2025).
- [50] M. Tanaka, Y. Yamaguchi and M. Harada, *Phys. Rev. D* **110**, 016024 (2024).
- [51] H.H. He, M.J. Yan, C.S. An and C.R. Deng, *Phys. Rev. D* **111**, 094038 (2025).
- [52] C.R. Deng, H. Chen and J.L. Ping, *Eur. Phys. J. A* **56**, 9 (2020).
- [53] A. Ali, Q. Qin, and W. Wang, *Phys. Lett. B* **785**, 605 (2018).
- [54] A. De Rujula, H. Georgi and S.L. Glashow, *Phys. Rev. D* **12**, 147 (1975).
- [55] N. Isgur and G. Karl, *Phys. Rev. D* **18**, 4187 (1978).
- [56] N. Isgur and G. Karl, *Phys. Rev. D* **20**, 1191 (1979).
- [57] D.A. Liberman, *Phys. Rev. D* **16**, 1542 (1977).
- [58] V.G. Neudachin, Y.F. Smirnov and R. Tamagaki, *Prog. Theor. Phys.* **58**, 1072 (1977).
- [59] Y. Fujiwara and K.T. Hecht, *Nucl. Phys. A* **444**, 541 (1985).
- [60] M. Oka and K. Yazaki, *Nucl. Phys. A* **402**, 477 (1983) [erratum: *Nucl. Phys. A* **458**, 773 (1986)].
- [61] A. Manohar and H. Georgi, *Nucl. Phys. B* **234**, 189 (1984).
- [62] I.T. Obukhovskiy and A.M. Kusainov, *Phys. Lett. B* **238**,

- 142 (1990).
- [63] F. Fernandez, A. Valcarce, U. Straub and A. Faessler, J. Phys. G **19**, 2013 (1993).
- [64] A. Valcarce, F. Fernandez, P. Gonzalez and V. Vento, Phys. Lett. B **367**, 35 (1996).
- [65] Y. Fujiwara, C. Nakamoto and Y. Suzuki, Phys. Rev. C **54**, 2180 (1996).
- [66] J. Vijande, F. Fernandez and A. Valcarce, J. Phys. G **31**, 481 (2005).
- [67] M.D. Scadron, Phys. Rev. D **26**, 239 (1982).
- [68] F. James and M. Roos, Comput. Phys. Commun. **10**, 343 (1975).
- [69] B. Silvestre-Brac and C. Gignoux, Phys. Rev. D **32**, 743 (1985).
- [70] B. Silvestre-Brac, Few Body Syst. **20**, 1 (1996).
- [71] E. Hiyama, Y. Kino and M. Kamimura, Prog. Part. Nucl. Phys. **51**, 223 (2003).
- [72] L. Meng, Y.K. Chen, Y.Ma and S.L. Zhu, Phys. Rev. D **108**, 114016 (2023).
- [73] M. Nzar and P. Hoodbhoy, Phys. Rev. C **42**, 1778 (1990).